Optoelectronic properties of polymer-nanocrystal composites active at near-infrared wavelengths

Olga Solomeshch, Ariel Kigel,[a] Aldona Saschiuk,[a] Vlad Medvedev, Assaf Aharoni,[b] Alexey Razin, Yoav Eichen,[a] Uri Banin,[b] Efrat Lifshitz,[a] and Nir Tessler[c]
Nanoelectronic Center, Electrical Engineering Department, Technion, Haifa 32000, Israel

(Received 14 February 2005; accepted 22 August 2005; published online 12 October 2005)

We report a systematic study of the optoelectronic processes occurring in composites made of near-infrared (IR) emitting nanocrystals and conjugated polymers. We focus on PbSe and InAs/ZnSe blended with polyphenylenevinylene-type polymers. We find that the process responsible for quenching the visible luminescence of the polymer by the nanocrystal varies depending on the nanocrystal composite. Moreover, the high (66%) energy-transfer efficiency from the polymer to the PbSe nanocrystal does result in significant emission at the near IR. Our measurements suggest that the host may be doping the PbSe nanocrystal, thus making the nonradiative Auger process favorable. For InAs we find the energy levels well aligned inside the polymer band gap, making it an efficient charge trap which acts as a luminescence center. Through two-dimensional numerical modeling of the charge transport in such composite films we highlight the importance of morphology (nanocrystal distribution) control. © *2005 American Institute of Physics*. [DOI: 10.1063/1.2064307]

I. INTRODUCTION

Semiconducting (conjugated) organic molecules and polymers[1,2] are now reaching the market in the form of full color (small size) displays. This implies that a certain level of material quality as well as understanding of device operation [e.g., light-emitting diode (LED)] has been achieved.[3,4] While this class of materials is highly attractive for a range of applications, it is clear that the properties of these materials are not as broad as one may wish. In parallel, molecular size inorganic nanocrystals[5] (NCs) based on a range of materials[6–10] have been developed. Naturally, the above two types of "molecular" materials have been used together in the form of blends (sometime solid solutions) in order to extend the mechanical, optical, and electrical properties of each family. To this end, organic-inorganic nanocomposites are being developed to produce composite visible light-emitting diodes[11–13] and efficient solar cells,[14,15] all active in the visible range. The extension of organic LEDs into the technologically important near-infrared (near-IR) spectral range used in telecommunications is gaining increased attention typically using lanthanide complexes[16,17] and inorganic nanocrystals.[18–20] Recently, we have reported an efficient electroluminescence[18] at the near infrared (and above 1 μm) based on InAs NCs and conjugated polymer hosts. This was followed by a report of efficient emission based on PbS (Ref. 19) NCs and a less-efficient emission based on PbSe.[20] This paper discusses an investigation of LED structures comprised of InAs/ZnSe (core-shell) and PbSe (core) NCs and polyphenylenevinylene (PPV)-type polymers, focusing on the following controlling parameters: (a) energy or charge-transfer process between the host polymer and the embedded nanocrystals, examined by quenching/enhancement of the photoluminescence (PL) and PL-excitation intensity of either one of the constituents, (b) determination of the relative energy levels of the constituents, using cyclic voltammetry measurements, and (c) the effect of charge trapping at the nanocrystalline site, on the LED performance, using a numerical model. These results suggest that the materials' composition (polymer and nanocrystals) has a crucial influence on the electroluminescence process.

II. EXPERIMENT

A. Synthesis and basic properties

Core/shell InAs/ZnSe NCs with an average core radius of 2.4 nm InAs and a ZnSe shell with a nominal thickness of 1.5 monolayers with strong emission in the 1.3–1.5 μm range were prepared in a two-step synthesis as reported previously.[7,21] PbSe core and PbSe/PbS core-shell NCs, emitting in the 1.2–1.8 μm spectral range, were prepared according to the procedure given in Refs. 10 and 22. Schematic drawing of the polymer constituents, MEH-PPV or yellow-PPV,[23] and the aforementioned NCs are drawn in Fig. 1. Separate solutions of the polymer and NCs, each dissolved in toluene, were prepared initially. These solutions were then mixed at the required NC-to-polymer volume ratio. Finally, the optical absorption of the composite film was measured and used as a final monitor. Optically homogeneous films were spin casted from solution to ~100 nm thickness onto a suitable substrate.

Representative absorption and PL spectra of the NC constituents, recorded at room temperature, with various NC sizes are shown in Fig. 2(a). These spectra reflect the tunability in the near-IR spectral regime and the high quality of

[a]Department of Chemistry and Solid-State Institute, Technion, Haifa 32000, Israel.
[b]Institute of Chemistry and the Center for Nanoscience and Nanotechnology, The Hebrew University of Jerusalem, Jerusalem 91904, Israel.
[c]Electronic mail: nir@ee.technion.ac.il; website: www.ee.technion.ac.il/nir

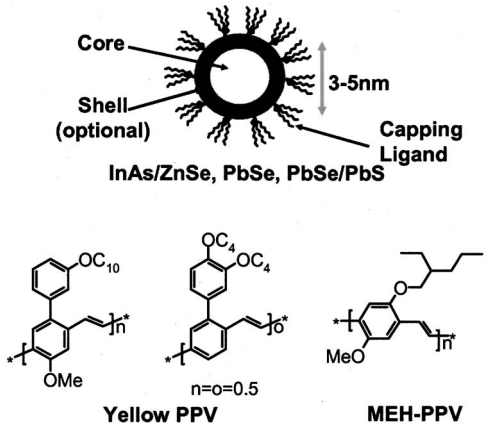

FIG. 1. Schematic description of the nanocrystals and polymers used in this study. The nanocrystal is described as having a core (as InAs or PbSe), optional shell (as ZnSe or PbS), and a solubilizing organic ligand.

the NCs. Comparison of the absorption spectra of the pure polymer and polymer-NC composites is given in Fig. 2(b). The dashed line in Fig. 2(b) designates the absorption of the NCs (in polystyrene matrix), the dashed-dotted line denotes the pristine PPV, while the full line shows the PPV-NC composite film. The absorption of the composite is essentially a combination of the two constituents. The bands between 800 and 1600 nm correspond to the quantum-confined transitions of the NCs (the absorption of the first excited state is enlarged), and those below 600 nm are associated with the host conjugated polymer overlapping the high-energy side of the NC absorption. The representative absorption spectra in Fig. 2(b) were used to calibrate/monitor the relative content of the NC to PPV.

Thus, Fig. 2 demonstrated the advantages in blending InAs/ZnSe, PbSe, and PbS NCs into a polymer host, extending the tunability across the telecommunication band, improving the process ability and device manufacturing technology of organic LEDs. Figure 3 shows the PL quantum efficiency of yellow PPV as a function of InAs/ZnSe and PbSe NC loading. Both NC materials quench the luminescence of the host in an effective manner. The quenching of the host emission suggests that there may be an efficient

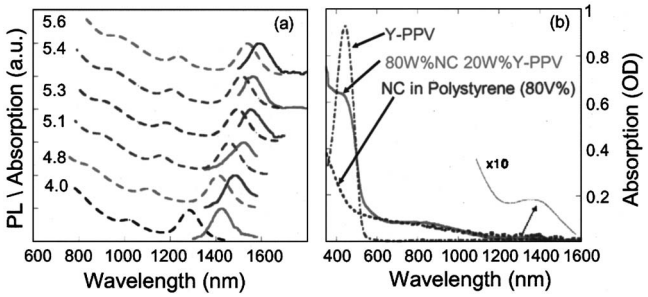

FIG. 2. (a) Absorption (dashed) and emission (full line) spectra of different size PbSe nanocrystals. The base line is shifted for clarity. (b) Absorption spectrum of the nanocrystals in polystyrene matrix (dashed line), of the pristine PPV (dashed dotted line), and of the PPV-NC composite (solid line). The magnified absorption at about 1400 nm shows the first excited state of the NC (embedded in PPV). The nanocrystals used in this subfigure are InAs/ZnSe and the polymer is superyellow PPV. However, similar features are found for composites containing PbSe or other PPV derivatives.

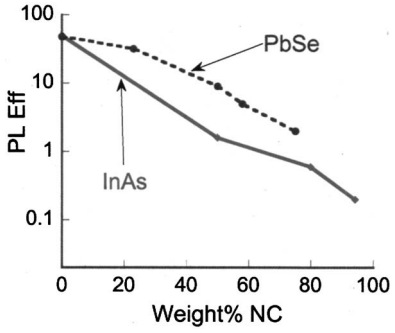

FIG. 3. PL quantum efficiency of yellow PPV as a function of nanocrystal loading.

energy transfer to the guest NC; thus the blends are potentially attractive for electroluminescence at the near IR.

B. Electroluminescence

While the general features of InAs/ZnSe and PbSe NCs look very similar, the performance as light-emitting diodes is very different. Figure 4(a) represents a plot of a light-current characteristic at the near infrared (left abscissa) and the external efficiency (right abscissa) of InAs/ZnSe (80 wt %) in the PPV host LED. The luminescence was measured through a 1-μm-high pass filter. The response is linear and the external efficiency increases rapidly, reaching a maximum value of 0.5% (Ref. 18) at the highest applied current. Figure 4(b) shows the emission spectra measured under optical (PL, solid line) and electrical (EL, symbols) excitations of the InAs/ZnSe-PPV composite.

Figure 4(c) shows the light-current characteristics at the near IR of PbSe embedded in yellow-PPV LEDs. The re-

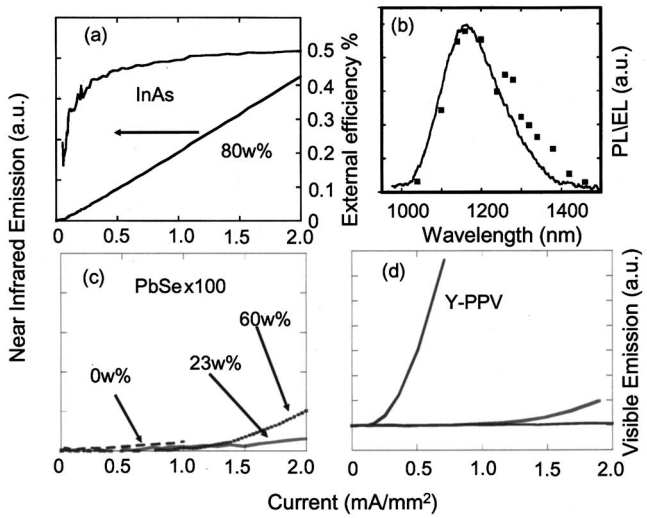

FIG. 4. (a) Near-IR light emission as a function of the applied current for InAs/ZnSe-PPV composite LED. The solid line shows the emission power (a.u.) and the dashed line shows the calculated external efficiency. (b) PL (solid line) and EL (symbols) spectrum of InAs/ZnSe-PPV composite. (c) Near-IR light emission as a function of the applied current for PbSe-PPV LEDs have 0 wt % PbSe (dashed), 23 wt % PbSe (solid), and 60 wt % PbSe in PPV (dot dashed). (d) Visible light emission as a function of the applied current for the same PbSe-PVV LEDs as in (c). Note that despite the strong quenching of the visible electroluminescence there is no emission, from the PbSe, at the near IR.

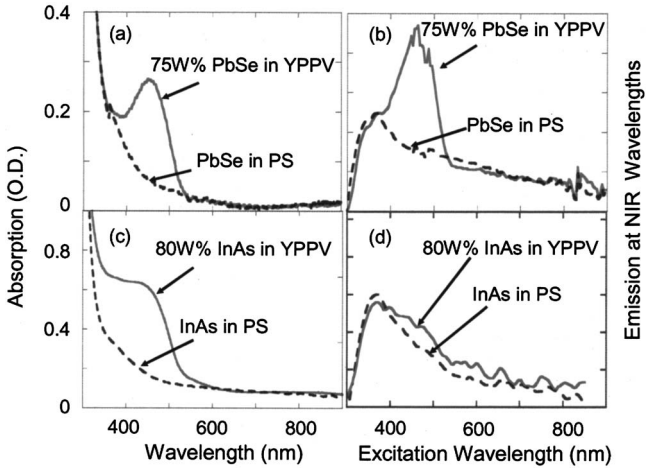

FIG. 5. (a) Absorption spectrum of PbSe NCs in polystyrene (dashed) and in yellow PPV (full line). (b) Excitation spectrum of PbSe NCs in polystyrene (dashed line) and in yellow PPV (full line). (c) Absorption spectrum of InAs/ZnSe NCs in polystyrene (dashed) and in yellow PPV (full line). (d) Excitation spectrum of InAs/ZnSe NCs in polystyrene (dashed line) and in yellow PPV (full line).

sponse of the pristine PPV is given by the dashed line, representing the base line "noise" of the system. The dash-dotted and full lines correspond to 23 and 60 wt % PbSe NCs in yellow PPV, respectively. We note that the measured near-IR emission of the PbSe-NC–polymer blend barely goes above the noise level and indeed the efficiency at the near IR is negligibly small, in agreement with Steckel *et al.*[20] The light-current characteristic of the visible emission of the host is plotted in Fig. 4(d), without (dashed) and with (dash-dotted and full lines) PbSe NCs. We note that the presence of PbSe quenches the electroluminescence of the yellow-PPV host, in agreement with Fig. 3. However, as is shown in Fig. 4(c), no significant electroluminescence was detected at the near IR for the PbSe compound.

C. Energy and charge-transfer paths

The light-current characteristics discussed above do not elucidate whether the quenching of the host electroluminescence is associated with an efficient energy transfer from the polymer host to the NC guests [as suggested by Fig. 3(b)] or due to other channels (e.g., chemical hindrance). This issue was further clarified by the examination of the PL-excitation and absorption spectra of PbSe and InAs/ZnSe NCs blended with yellow PPV (YPPV), in comparison with the spectra of those NCs dispersed in polystyrene (PS) (acting as an optically inert polymer). Figure 5(a) shows the absorption spectrum of the PbSe-NC/YPPV (full line) and PbSe-NC/PS (dashed line) films. A complementary measurement is shown in Fig. 5(b) which describes their PL-excitation spectra, monitored at the PbSe emission spectral regime [see Fig. 2(a)]. The spectrum corresponding to the PbSe-NC/PS film was normalized to overlap that of the PbSe-NC/YPPV film outside the main absorption band of the YPPV. Examining Fig. 5(a) and comparing the dashed and full lines we find that at the absorption band of the composite (centered at 450 nm) the direct absorption by the NCs contributes 25% to the total absorption and only 75% is due to the YPPV absorption. Let us now turn to Fig. 5(b) which shows the PL-excitation spectra of the discussed films recorded between 300 and 900 nm. The solid and dashed lines describe the excitation spectrum of PbSe-NC/YPPV and of PbSe-NCs/PS, respectively (the reduction of the signal close to 300 nm is an instrumental artifact). Again, the spectrum corresponding to the PbSe-NC/PS film was normalized to overlap that of PbSe-NC/YPPV film outside the main excitation band of the YPPV. Comparing the dashed and full lines we find that at the onset of the YPPV absorption there is enhanced emission from the PbSe NCs, indicating an energy transfer from the YPPV host to the PbSe-nanocrystal guests. Comparison of the relative intensities of the PL excitation at 450 nm of the two films reveals a contribution of 66% due to energy transfer from the YPPV and 34% contribution due to direct excitation of the PbSe NCs (dashed line). Based on the data presented in Figs. 5(a) and 5(b), the energy-transfer efficiency is estimated as $\mathrm{Eff}_{(\mathrm{PbSe})}=(0.66/0.34)/(0.75/0.25)=0.64$, showing there is efficient energy transfer from the YPPV to the PbSe NCs.

TABLE I. Near-IR photoluminescence efficiency in solution and in solid matrix.

	PL QE in toluene (%)	PL QE in matrix (%)
PbSe	50	2–5
InAs/ZnSe	20	N.A.

Next, we examine the InAs/ZnSe-based films [Figs. 5(c) and 5(d)]. Based on Fig. 5(c) the absorption of the YPPV polymer at 450 nm is 78% and that of the InAs/ZnSe NC is 22%. Figure 5(d), however, shows very little enhanced emission at 450 nm due to the absorption by the polymer. Comparing the two spectra in Fig. 5(d) we find that the energy transfer from the polymer contributes about 20% to the total emission. Again we can estimate the efficiency of the energy-transfer process as $\mathrm{Eff}_{(\mathrm{InAs})}=(0.2/0.8)/(0.78/0.22)=0.07$, showing that the energy transfer from YPPV to the InAs/ZnSe NCs is much less efficient than that of the energy transfer to the PbSe nanocrystals. However, the overall photoluminescence at the near infrared was weak for both PbSe- and InAs/ZnSe-based films. Quantitative measure of the emission efficiency was carried out by using integrating sphere measurements[24] of the photoluminescence quantum yield (PLQY) of PbSe in solution and in a YPPV matrix (see Table I). To avoid complication associated with energy transfer the excitation wavelength was chosen to be close to 900 nm where the YPPV does not absorb. The PLQY of PbSe in solution and in the YPPV matrix was 50% and 3%, respectively.

Hence, the above set of results seems puzzling and it conveys the following intermediate conclusions: The embedded NCs, both of InAs/ZnSe and PbSe, quenched the electroluminescence of the PPV hosts. In the case of PbSe this quenching was probably associated with an efficient energy transfer from the YPPV host to the PbSe NCs but in the case of the InAs/ZnSe NCs no such energy transfer is expected. On the other hand, the quenching of the host electrolumines-

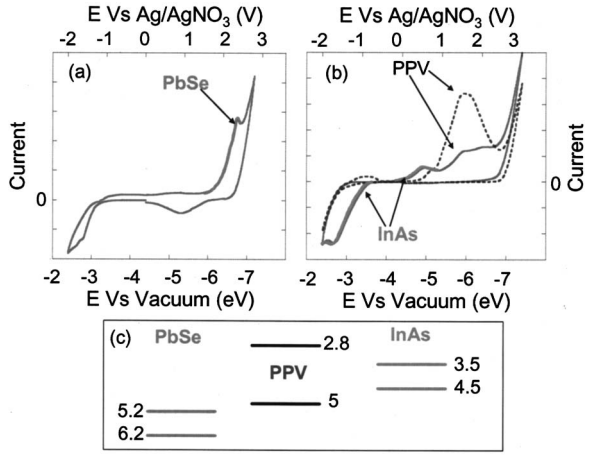

FIG. 6. CV curves of spin-coated films on an ITO substrate. (a) PbSe in polystyrene matrix; (b) pristine PPV (dashed line) and InAs/PPV composite (solid line); (c) schematic description of the energy levels based on the CV measurements.

cence is accompanied by an impressive enhancement of the electroluminescence in the near IR when embedded with InAs/ZnSe NCs, and negligible electroluminescence for PbSe NCs. Therefore, it is presumed that the InAs/ZnSe NCs are excited through a charge-transfer process from the YPPV, rather than an energy-transfer process.

To elucidate the above differences between the PbSe- and InAs/ZnSe-based LEDs we conducted cyclic voltammetry (CV) measurements that would reveal the relative energy-level alignment. The NC/polymer solutions were spin coated over ITO substrates, acting as working electrode. The samples were examined in a cell containing $0.1M$ tetrabutylammonium hexafluorophosphate ($TBAPF_6$) in anhydrous acetonitrile as supporting electrolyte. Platinum wire was used as a counterelectrode and $Ag/AgNO_3$ ($0.01M$ in acetonitrile) as a reference electrode (with scan speed=0.1 V/s). The sample preparation and CV measurements were carried out in an inert atmosphere (N_2) glove box. Figure 6(a) shows the measured CV curves of PbSe and Fig. 6(b) shows the measured CV curves for InAs (core only) in a PPV matrix (full line) and of the pristine PPV (dashed line). Note that the signal for the InAs/PPV composite films shows contributions from both the InAs and the YPPV. The signal for the pristine PPV film helps us identify the signal associated with InAs only in the composite film (see figure). The onset potentials (E_{ox} and E_{red}) of p and n doping are used to determine the highest occupied molecular orbital (HOMO) and lowest unoccupied molecular orbital (LUMO) energy levels by means of the empirical relationship proposed in Ref. 25. This relationship connects the solid-state ionization potential (IP) (HOMO energy) and electron affinity (EA) (LUMO energy) to the E_{ox} and E_{red} using the relations IP $(E_{HOMO})=-(E_{ox}+4.4)$ (eV) and EA $(E_{LUMO})=-(E_{red}+4.4)$ (eV), where E_{HOMO} and E_{LUMO} are the HOMO and LUMO energy levels below the vacuum. The value of 4.4 at the indicated relations corresponds to the difference between the vacuum level potential of the saturated calomel electrode (SCE) and the potential of the $Ag/AgNO_3$ electrode. As often found, the HOMO level is better resolved, while the LUMO level is

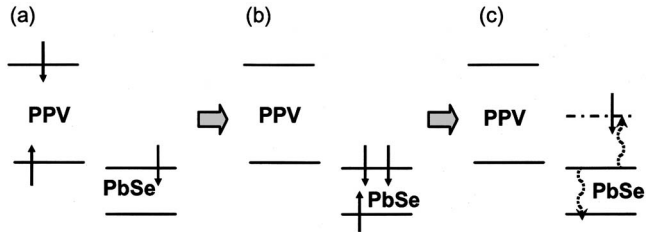

FIG. 7. (a) First step—part of the light is absorbed by the polymer and part directly on the NC. (b) Second step—energy transfer from polymer to NC followed by efficient quenching to the ground state (c).

deduced from the optical-absorption gap. Figure 6(c) shows schematically the energy-level position of the materials used in this study. We note that while InAs is positioned inside the polymer gap the levels of PbSe are shifted to much lower energies with the LUMO level being at ~5.2 eV below the vacuum level.

The position of the InAs levels within the PPV band gap suggests that it is an efficient charge trap for both electrons and holes. Namely, the high efficiency in the InAs/ZnSe-based LEDs is a result of efficient charge transfer that compensates for the poor energy transfer. The levels of the PbSe, however, are positioned outside the PPV band gap. Since the LUMO of PbSe is so low compared to the vacuum level it will be below the Fermi level of most common organic hosts and an electron transfer from the polymer HOMO to the PbSe (doping) is energetically favored. This implies that within the PbSe-NC/PPV composite, the optical excited state of the PbSe will be similar to that of an N-doped semiconductor with two electrons and one hole. In this case the most probable decay channel is the nonradiative Auger process.[26] Indeed Table I indicates a poor luminescence efficiency of the PbSe NCs within the NC/polymer composite while Fig. 5(b) revealed an efficient energy-transfer process from the polymer into the PbSe NCs. A proposed mechanism is drawn schematically in Fig. 7. Figure 7(a) shows a polymer molecule absorbing a photon and a nanocrystalline energy level having one electron in the LUMO level (N-doped species). Following the excitation of the polymer host the energy is transferred [Fig. 7(b)] to the PbSe guest. The presence of two electrons and a hole initiate the Auger process [Figure 7(c)], creating a single hot electron (that will consequently relax nonradiatively to the PbSe LUMO level).

Considering the above physical picture, we presume that efficient LED performance in the near IR can be maintained when the polymer's HOMO level is below the nanocrystal's HOMO levels and the polymer's LUMO level is above the nanocrystal's one. Such energy-level alignment will preclude spontaneous donation of electron by the polymer (at room temperature). This condition is fulfilled for InAs and most polymer hosts and is NOT fulfilled for the PbSe nanocrystals studied here. In this context we note that our preliminary studies, focused on the preparation of PbSe/PbS core-shell and alloyed $PbSe/PbSe_xS_{1-x}$ NCs, offer the possibility to shift the HUMO and LUMO energy levels of the IV–VI semiconductor NCs, with respect to that of the polymer, and tune the exciton energy with variation of the NC size, as well

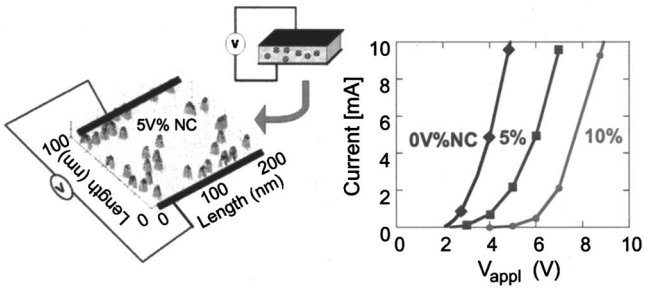

FIG. 8. Left: schematic description of the device structure used for the 2D transport modeling. The "bumps" denote the deep wells in the valence band representing the nanocrystals. Right: simulated *I-V* curve for pristine PPV (diamonds), 5 vol % of NC (squares), and 10 vol % of NC in a PPV matrix (circles). The effect of the NC was calculated for an effective well depth of 0.3 eV.

as their composition.[10] These NCs will be used in the near future for the preparation of PbSe NC/PPV-based LEDs and will be published elsewhere.

III. DEVICE PERFORMANCE AND MODELING

The role of carriers' trapping and its importance for improving device design and modeling is emphasized in this section.[27] We use a two-dimensional (2D) simulation which solves Eqs. (1)–(3) below self consistently:

$$\nabla E = -\frac{q}{\varepsilon_\pi \varepsilon_0} p, \tag{1}$$

$$J = qp\mu E + qD\nabla p, \tag{2}$$

$$\frac{\partial}{\partial t} p(t) = \frac{1}{q}\nabla J = \nabla[D_n \nabla p(t) + \mu p(t) E(t)]. \tag{3}$$

Equation (1) is the Poisson equation, Eq. (2) is the current equation, and Eq. (3) is the current continuity equation (more details regarding device modeling can be found in Ref. 28). The NCs are modeled as deep wells, and for simplicity, we considered only one charge carrier. Namely, the presence of the NC is modeled as a local shift (discontinuity) of the HOMO level (see Fig. 8).

The left side of Fig. 8 shows a 2D description of the device used in the model. The figure schematically shows the valence level of a composite, containing 5% NCs in volume, where shift of the HOMO level at the NC position creates a "bumplike" (inverse well) shape. The right side of Fig. 8 shows the calculated *I–V* curve as a function of NCs' loading. The figure exhibit a shift in the turn-on voltage,[18] typical of traplike regions (i.e., the wells). The charge-density distribution, calculated for a volume of 5% NCs and 5 V applied bias is shown in Fig. 9, revealing the existence of a pillar at each NC position ("trap"), indicating the high charge density within the NCs. The figure also shows the effect of the random distribution of NCs, with regions occupied by "shadow" or "deep" traps and other empty regions. The empty regions effectively designate pinholelike regions as the current do not pass through any nanocrystal. Moreover, examining the contact area in Fig. 9 suggests that traps situated close to the contact suppress the charge injection, as the charge density in the polymer is very low at such regions. This low density is in contrast to the central region which exhibits a density profile typical of Ohmic injection into low mobility semiconductors.

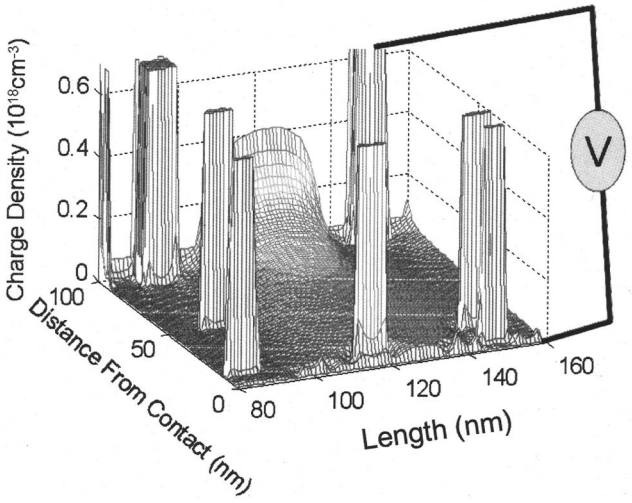

FIG. 9. Charge-density distribution inside a device. Note that the trapping on the NC influences not only the transport but only the transport but also the charge injection.

IV. CONCLUSIONS

To conclude, we have reported a systematic study of the properties of organic LEDs, based on PPV-PbSe and PPV-InAs/ZnSe composites active at the near infrared. The embedded NCs, both of InAs/ZnSe and PbSe, quenched the electroluminescence of the PPV hosts. This quenching was a result of an efficient energy transfer from the host into the PbSe NCs, and a charge transfer into InAs/ZnSe NCs. The quenching of the host luminescence is accompanied by an enhancement of the luminescence of InAs/ZnSe NCs, but by negligible luminescence of the PbSe NCs. The CV measurements suggested that an efficient LED performance in the near IR can be maintained when the polymer HOMO and LUMO levels wrap around the levels of the embedded NCs. This condition is fulfilled in the case of PPV-InAs NC composites and not for the PPV-PbSe composites. We suggest that modified PbSe NCs as the PbSe/PbS core-shell or alloyed PbSe/$PbSe_xS_{1-x}$ NCs, showing a shift in their HUMO and LUMO energy levels,[10] may be better suited for use in LED-type devices.

Finally, the experimental tools presented here enable to optimize the choice of multilayers and polymer/NC composition. The numerical model highlighted the need of optimizing the device structure, distribution of NCs, and possibly the need for multilayer design.

ACKNOWLEDGMENTS

We acknowledge support by the Israel Ministry of Science and Technology, partial support by the EU through Contract No. G5RD-CT-2001-00577 OPAMD, partial support from the Deutsche-Israel Program (DIP), and partial

support by the Niedersachsen foundation. We thank Avecia/Covion for the supply of the yellow PPV. Two of the authors (O.S. and A.S.) express deep gratitude to the Center of Absorption in Science, Ministry of Absorption, Israel.

[1]A. J. Heeger, Rev. Mod. Phys. **73**, 681 (2001).
[2]R. H. Friend *et al.*, Nature (London) **397**, 121 (1999).
[3]B. K. Crone, P. S. Davids, I. H. Campbell, and D. L. Smith, J. Appl. Phys. **87**, 1974 (2000).
[4]Y. Preezant and N. Tessler, J. Appl. Phys. **93**, 2059 (2003).
[5]A. D. Yoffe, Adv. Phys. **50**, 1 (2001).
[6]B. O. Dabbousi, J. Rodriguez Viejo, F. V. Mikulec, J. R. Heine, H. Mattoussi, R. Ober, K. F. Jensen, and M. G. Bawendi, J. Phys. Chem. B **101**, 9463 (1997).
[7]Y. W. Cao and U. Banin, Angewandte Chemie-International **38**(24), 3692 (1999).
[8]H. Du, C. L. Chen, R. Krishnan, T. D. Krauss, J. M. Harbold, F. W. Wise, M. G. Thomas, and J. Silcox, Nano Lett. **2**, 1321 (2002).
[9]E. Lifshitz, M. Bashouti, V. Kloper, A. Kigel, M. S. Eisen, and S. Berger, Nano Lett. **3**, 857 (2003).
[10]M. Brumer, A. Kigel, L. Amirav, A. Sashchiuk, O. Solomesch, N. Tessler, and E. Lifshitz, Adv. Funct. Mater. **15**(7), 1111 (2005).
[11]V. L. Colvin, M. C. Schlamp, and A. P. Alivisatos, Nature (London) **370**, 354 (1994).
[12]M. C. Schlamp, X. G. Peng, and A. P. Alivisatos, J. Appl. Phys. **82**, 5837 (1997).
[13]S. Coe, W. K. Woo, M. Bawendi, and V. Bulovic, Nature (London) **420**, 800 (2002).
[14]N. C. Greenham, X. G. Peng, and A. P. Alivisatos, Phys. Rev. B **54**, 17628 (1996).
[15]W. U. Huynh, J. J. Dittmer, and A. P. Alivisatos, Science **295**, 2425 (2002).
[16]L. H. Slooff, A. Polman, F. Cacialli, R. Friend, G. Hebbink, F. van Veggel, and D. Reinhoudt, Appl. Phys. Lett. **78**, 2122 (2001).
[17]R. J. Curry and W. P. Gillin, Appl. Phys. Lett. **75**, 1380 (1999).
[18]N. Tessler, V. Medvedev, M. Kazes, S. H. Kan, and U. Banin, Science **295**, 1506 (2002).
[19]L. Bakueva, S. Musikhin, M. A. Hines, T. W. F. Chang, M. Tzolov, G. D. Scholes, and E. H. Sargent, Appl. Phys. Lett. **82**, 2895 (2003).
[20]J. S. Steckel, S. Coe-Sullivan, V. Bulovic, and M. G. Bawendi, Adv. Mater. (Weinheim, Ger.) **15**, 1862 (2003).
[21]Y. W. Cao and U. Banin, J. Am. Chem. Soc. **122**, 9692 (2000).
[22]C. B. Murray, S. H. Sun, W. Gaschler, H. Doyle, T. A. Betley, and C. R. Kagan, IBM J. Res. Dev. **45**, 47 (2001).
[23]H. Becker, H. Spreitzer, W. Kreuder, E. Kluge, H. Schenk, I. Parker, and Y. Cao, Adv. Mater. (Weinheim, Ger.) **12**, 42 (2000).
[24]J. C. deMello, H. F. Wittmann, and R. H. Friend, Adv. Mater. (Weinheim, Ger.) **9**, 230 (1997).
[25]D. M. deLeeuw, M. M. J. Simenon, A. R. Brown, and R. E. F. Einerhand, Synth. Met. **87**, 53 (1997).
[26]V. I. Klimov, A. A. Mikhailovsky, D. W. McBranch, C. A. Leatherdale, and M. G. Bawendi, Science **287**, 1011 (2000).
[27]A. Shik, S. Yu, E. Johnson, H. Ruda, and E. H. Sargent, Solid-State Electron. **46**, 61 (2002).
[28]S. Selberherr, *Analysis and Simulation of Semiconductor Devices* (Springer, Vien, 1984).